

Scaling of the spin stiffness in random spin- $\frac{1}{2}$ chains

Crossover from pure-metallic behaviour to random singlet-localized regime

Nicolas Laflorencie¹ and Heiko Rieger²

¹ Laboratoire de Physique Théorique, CNRS-UMR5152 Université Paul Sabatier, F-31062 Toulouse, France

² Theoretische Physik; Universität des Saarlandes; 66041 Saarbrücken; Germany

March 20, 2019

Abstract. In this paper we study the localization transition induced by the disorder in random antiferromagnetic spin- $\frac{1}{2}$ chains. The results of numerical large scale computations are presented for the XX model using its free fermions representation. The scaling behavior of the spin stiffness is investigated for various disorder strengths. The disorder dependence of the localization length is studied and a comparison between numerical results and bosonization arguments is presented. A non trivial connection between localization effects and the crossover from the pure XX fixed point to the infinite randomness fixed point is pointed out.

PACS. XX.XX.XX No PACS code given

1 Introduction

Quantum spin chains exhibit a large number of interesting features because the quantum fluctuations are often relevant, especially at low temperature. The antiferromagnetic (AF) Heisenberg model in one dimension (1D) has been extensively studied since the discovery in 1931 of the Bethe Ansatz [1] for the spin $S = \frac{1}{2}$ chain. In 1D, the AF XXZ model defined by the Hamiltonian

$$\mathcal{H}^{XXZ} = J \sum_{i=1}^L \left[\frac{1}{2} (S_i^+ S_{i+1}^- + \text{h.c.}) + \Delta S_i^z S_{i+1}^z \right] \quad (1)$$

with $J > 0$ and $\Delta \geq 0$, exhibits a gap-less excitation spectrum for $S = \frac{1}{2}$ if $\Delta \leq 1$, whereas a gap opens up in the spectrum when $\Delta > 1$. In 1D, the quantum fluctuations prevent the formation of true long-range order [2] but in the critical regime $\Delta \leq 1$ the model [Eq.(1)] displays a *quasi*-long-range order (QLRO) with power-law decaying spin-spin correlation functions in the ground state (GS). It is well known that the model [Eq.(1)], without quenched disorder, is integrable for conventional periodic boundary conditions [1] as well as in the more general case of twisted boundary conditions (TBC) [3]. The latter are defined by:

$$S_{L+1}^z = S_1^z, \quad S_{L+1}^\pm = S_1^\pm e^{\pm i\phi}, \quad (2)$$

where ϕ is the twist angle and is equivalent to a ring of interacting fermions threaded by a magnetic flux of strength $\frac{\hbar c}{e} \phi$ [4]. The spin stiffness ρ_S is defined by

$$\rho_S = L^2 \frac{\partial^2 \epsilon_0(\phi)}{\partial \phi^2} \Big|_{\phi=0}, \quad (3)$$

where ϵ_0 is the GS energy per site. It measures the magnetization transport along the ring and in the fermionic language this is called the charge stiffness, which is the Drude weight of the conductivity. The gap-less phase is characterized by peculiar transport properties: in the thermodynamic limit Shastry and Sutherland [5] showed that in the critical regime the spin stiffness of the XXZ chain follows:

$$\rho_S(\Delta) = J \frac{\pi \sin(\mu)}{4\mu(\pi - \mu)} \quad \text{where } \Delta = \cos(\mu), \quad (4)$$

and it vanishes for $\Delta > 1$. The phase transition which occurs at $\Delta = 1$ can be viewed as a metal-insulator transition [5] between a critical metallic phase with a finite ρ_S and a gaped insulating regime where $\rho_S = 0$, following a *Mott* mechanism.

When the system is not homogeneous, the situation described above changes dramatically. For instance when only one coupling exchange is weaker than the others in an otherwise homogeneous ring, the stiffness has been found to scale to zero by numerical studies [6], in perfect agreement with renormalization group arguments of Eggert and Affleck [7], and Kane and Fisher [8].

Moreover, for the case of a random spin- $\frac{1}{2}$ chain, Doty and Fisher [9] performed a bosonization study considering several types of random perturbations added to (1). They concluded that in the AF critical regime the GS with QLRO is destroyed by any small amount of disorder and the phase transition associated is an *Anderson* localization transition [10], reminiscent of the localization problem in 1D disordered metals studied by Giamarchi and Schulz [11]. A relevant length scale associated with the Anderson

transition is the localization length ξ^* .

More generally, the problem of transport in 1D random media [15] as well as localization effects and persistent currents in disordered quantum rings have motivated a large number of theoretical studies in recent years [16, 17, 18, 19, 20, 21]. In the context of mesoscopic physics it turned out to be very interesting to study the transport properties for finite systems, where coherence effects are important [22, 23]. In particular the finite size (FS) dependence of the current, susceptibility and stiffness are important for a complete understanding of the experimental results.

In the present paper we investigate the scaling behavior of the spin stiffness of the random spin- $\frac{1}{2}$ chain. It is organized as follows. In Sec. 2, the numerical method, based on the free fermions formalism, is explained and notably the computation of the spin stiffness is described. Sec. 3 is devoted to the study of the localization transition: Using some bosonization arguments as well as FS scaling analysis, an universal scaling of the stiffness to 0 is expected and we compare it with numerical results. In Sec. 4, the disorder dependence of the localization length is studied and the bosonization predictions are demonstrated to be valid only for weak randomness. For strong disorder we propose a new quantity which gives a better description for the disorder dependence of ξ^* . The relation to crossover effects observed recently for spin-spin correlation functions [12, 13] is also worked. Sec. 5 contains some concluding remarks.

2 Numerical method at the XX point

We start with the 1D random XX model on a ring closed with TBC. It is defined by

$$\mathcal{H}_{\text{random}}^{XX}(\phi) = \sum_{i=1}^{L-1} \left[\frac{J_i}{2} (S_i^+ S_{i+1}^- + \text{h.c.}) \right] + h_L(\phi), \quad (5)$$

with the boundary term $h_L(\phi) = \frac{J_L}{2} (S_L^+ S_1^- e^{-i\phi} + \text{h.c.})$. The couplings J_i are independent random numbers.

2.1 Free fermions formulation

For $S = \frac{1}{2}$ the well known Jordan-Wigner mapping transforms spin operators into Fermi operators according to

$$S_j^+ = C_j^\dagger e^{i\pi \sum_{i=1}^{j-1} N_i}, \quad S_j^- = e^{-i\pi \sum_{i=1}^{j-1} N_i} C_j. \quad (6)$$

$N_j = C_j^\dagger C_j$ is the occupation number (0 or 1) at site j , given by $N_j = 1/2 + S_j^z$. Note that the Fermi anti-commutation relations are satisfied $\{C_i^\dagger, C_j\} = \delta_{i,j}$. The Hamiltonian (5) can then be written as

$$\mathcal{H}_{\text{random}}^{XX}(\phi) = \sum_{i=1}^{L-1} \left[\frac{J_i}{2} (C_i^\dagger C_{i+1} + C_{i+1}^\dagger C_i) \right] + h_L(\phi). \quad (7)$$

The sign of the boundary term depends on the parity of the total number of fermions $\mathcal{N} = \sum_{i=1}^L N_i$; indeed

$$h_L(\phi) = -e^{i\pi \mathcal{N}} \frac{J_L}{2} (C_L^\dagger C_1 e^{-i\phi} + C_1^\dagger C_L e^{i\phi}). \quad (8)$$

Hence, when $\phi = 0$ the resulting free fermions problem must have anti-periodic boundary conditions if the number of fermions is even and periodic boundary conditions if \mathcal{N} is odd [24]. In the non-random case, the solution of the problem via a Fourier transformation is trivial [25] due to its translational invariance. In k -space, the pure model is given by

$$\mathcal{H}_{\text{pure}}^{XX} = -J \sum_k C_k^\dagger C_k \cos(k). \quad (9)$$

Its GS is at half-filling ($\mathcal{N} = \frac{L}{2}$, corresponding to the $S_{\text{tot}}^z = 0$ sector). The twist angle at the boundary produces a shift in the momentum space $k \rightarrow k + \phi$ which can be uniformly distributed over all bond resulting in a local twist $\delta\phi = \frac{\phi}{L}$ for each bond. Therefore the GS energy per site takes the following simple expression

$$\epsilon_0(L, \phi) = -\frac{J}{L} \sum_p \cos\left(\frac{2\pi p}{L} + \frac{\phi}{L}\right) = -\frac{J \cos(\frac{\phi}{L})}{L \sin(\frac{\pi}{L})} \quad (10)$$

from which we can easily extract the spin stiffness [26] :

$$\rho_S(L) = J(L \sin(\frac{\pi}{L}))^{-1} \simeq \pi^{-1} + \mathcal{O}(L^{-2}). \quad (11)$$

When the system is inhomogeneous, the translational invariance is broken and a solution in the reciprocal space is no longer possible. Fortunately the problem can be easily diagonalized numerically, using standard linear algebra routines [27]. Indeed, with an unitary transformation the hamiltonian (7) can be expressed in a diagonal form [25, 24, 28, 29]. For completeness we give here a brief description of the method. First let us define a column vector Ψ of size L and its conjugate row vector Ψ^\dagger by

$$\Psi^\dagger = (C_1^\dagger, \dots, C_L^\dagger). \quad (12)$$

Hence, using this notation, we can re-write the Hamiltonian (7) in terms of a symmetric $L \times L$ band matrix $\mathcal{A}(\phi)$ as

$$\mathcal{H}_{\text{random}}^{XX}(\phi) = \Psi^\dagger \mathcal{A}(\phi) \Psi, \quad (13)$$

with non-zero elements given by $\mathcal{A}_{i,i+1} = \frac{J_i}{2}$ and at the boundaries, $\mathcal{A}_{1,L} = (-1)^{\mathcal{N}} \frac{J_L}{2} e^{-i\phi}$. One can define the unitary transformation P that diagonalizes \mathcal{A} . Then we get a new set of Fermi operators η_q defined by

$$\eta_q = \sum_i P_{iq} C_i, \quad \eta_q^\dagger = \sum_i P_{iq}^\dagger C_i^\dagger, \quad (14)$$

which yields the following diagonal form for the Hamiltonian

$$\mathcal{H}_{\text{random}}^{XX}(\phi) = \sum_{q=1}^L e_q(\phi) \eta_q^\dagger \eta_q, \quad (15)$$

where the $e_q(\phi)$ are the eigenvalues of $\mathcal{A}(\phi)$. At temperature T , the occupation number is given by the Fermi function $\langle N_q \rangle = \langle \eta_q^\dagger \eta_q \rangle = (1 + e^{e_q(\phi)/T})^{-1}$. Because of the particle-hole symmetry, the eigenvalues occur in pairs, equal in magnitude and opposite in sign. Hence, at $T = 0$, the GS energy is simply given by

$$\epsilon_0(\phi) = \sum_{q=1}^{N=L/2} e_q(\phi), \quad (16)$$

where $e_1(\phi) \leq e_2(\phi) \leq \dots \leq e_L(\phi)$.

2.2 Numerical evaluation of the spin stiffness

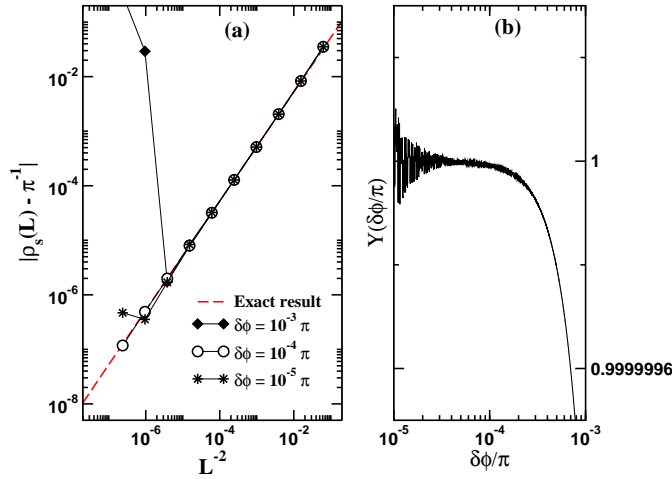


figure 1. (a) Magnitude of the FS corrections of the spin stiffness $|\rho_S(L) - \pi^{-1}|$ for different choices of the twist angle ϕ calculated for the pure XX model [Eq.(9)]. The long-dashed line is the exact result $L \sin(\frac{\pi}{L})^{-1} - \pi^{-1}$ and the different symbols show the numerical results for different values of the twist. (b) Function $Y(\delta\phi) = 2 \frac{1 - \cos(\delta\phi)}{(\delta\phi)^2}$ computed in double precision type.

Numerical estimates for the spin stiffness can be obtained by approximating Eq.(3) for finite L by

$$\rho_S \simeq 2 \frac{\epsilon_0(\phi) - \epsilon_0(0)}{(\delta\phi)^2}, \quad (17)$$

where $\delta\phi = \phi/L$ is the twist per site. Hence for a given system the calculation of ρ_S requires to compute Eq.(16) twice: once for finite ϕ and once for $\phi = 0$. Since the corrections are of order $1/L^2$ an extrapolation $L \rightarrow \infty$ is, in principle, straightforward and yields the desired result. However, the appropriate choice of ϕ is somewhat delicate as we show in Fig.1 (a). Here the numerical results for the FS scaling of the spin stiffness of the pure chain are depicted, computed for various system sizes ($L = 4, 8, 16, \dots, 2048$) with three different values of the twist angle, and compared to the exactly known result given by Eq.(11). The

discrepancy between the numerical data and the exact result, observed for $\delta\phi/\pi = 10^{-3}$ and $\delta\phi/\pi = 10^{-5}$ can be understood as follows. Using Eq.(10) one can rewrite Eq.(17) as

$$\rho_S \simeq 2 \frac{1 - \cos(\delta\phi)}{(\delta\phi)^2} J(L \sin \frac{\pi}{L})^{-1}. \quad (18)$$

The function $Y(\delta\phi) = 2 \frac{1 - \cos(\delta\phi)}{(\delta\phi)^2}$, which is exactly equal to one when $\delta\phi = 0$, is expected to decrease slowly when $\delta\phi$ increases. However, the numerical calculation of $Y(\delta\phi)$ is limited by the machine precision and therefore we observe in Fig.1 (b) that even in double precision type, for $\delta\phi/\pi < 10^{-4}$ undesirable oscillations appear. This puts a bound for the smallest value of $\delta\phi$ that is meaningful for our numerical procedure, as we demonstrate in Fig.1 (a) for $\delta\phi/\pi = 10^{-5}$. On the other hand, when $\delta\phi > 10^{-4}$ the value of Y deviates significantly from one as shown in Fig.1 (a) for $\delta\phi/\pi = 10^{-3}$. Therefore, for a numerical calculation in double precision, the numerical derivative Eq.(17) gives the most reliable results for $\delta\phi \simeq 10^{-4}\pi$ which is confirmed by the numerical data obtained in this case, shown in Fig.1 (a).

3 Localization transition : Scaling from pure to infinite randomness behavior

3.1 Bosonization predictions for weak disorder and scaling argument in the localized-random singlet phase

The critical behavior of the XXZ model [Eq.(1)] with weak randomness in the couplings and/or in external magnetic fields has been studied by Doty and Fisher [9] using a bosonization approach. They found that for random perturbations which preserve the XY symmetry, the critical properties belong to the universality class of Giamarchi-Schulz transition for 1D bosons in a random potential [11]. Let us define the disorder parameter \mathcal{D} by

$$\mathcal{D} = \overline{(J_i)^2} - \left(\overline{J_i} \right)^2. \quad (19)$$

For weak initial randomness $\mathcal{D}_0 \ll 1$, the renormalization of the disorder under a change of length scale $l = \ln L$ is [9, 11]

$$\frac{\partial \mathcal{D}}{\partial \ln L} = (3 - 2K)\mathcal{D}, \quad (20)$$

where K is the Δ -dependent Luttinger liquid parameter $K(\Delta) = \frac{\pi}{2(\pi - \mu)}$. Therefore, if $K < 3/2$ (i.e. $-\frac{1}{2} < \Delta < 1$) the disorder is a relevant perturbation and the line of pure fixed points is unstable under any amount of randomness. Under renormalization the system runs into an infinite randomness fixed point (IRFP) [9, 30]. Using a real space decimation procedure [30], Fisher reached the same conclusion and demonstrated analytically the existence of an attractive IRFP. Strictly speaking, at the IRFP the system is in the so-called random singlet phase (RSP) or in the fermionic language, the fermions are localized and

their transport properties are the ones of an insulator. For instance, the Drude weight is expected to be 0 in the thermodynamic limit $L \rightarrow \infty$. The renormalization flow is controlled by a disorder dependent length scale which emerges from Eq.(20), the localization length:

$$\xi^*(\mathcal{D}) \sim \mathcal{D}^{-\frac{1}{3-2\kappa}}. \quad (21)$$

In the thermodynamic limit the spin stiffness is finite in the QLRO phase (see Eq.(4)) and its FS scaling behavior is well known [26]. On the other hand, when $\mathcal{D} > 0$ we have $\rho_S(L, \mathcal{D}) \rightarrow 0$ and expect a scaling of the form

$$\rho_S(L, \mathcal{D}) = g\left(\frac{L}{\xi^*(\mathcal{D})}\right), \quad (22)$$

with g a universal function. Defining $x = L/\xi^*(\mathcal{D})$, one can consider 3 different regimes : (i) For $x \ll 1$, i.e. on small length scales, the systems appears to be delocalized with $g \simeq \pi^{-1}$. (ii) For $x \gg 1$, i.e. on large length scales, the system shows the asymptotic behavior of the IRFP and $g \rightarrow 0$. (iii) In the intermediate region $x \sim 1$, a crossover between the pure repulsive fixed point and the attractive IRFP occurs. Utilizing standard FS scaling arguments [31], one can predict the behavior of $g(x)$ in the asymptotic regime of the IRFP: ρ_S has dimension of inverse (length $^{d-2} \times \xi_\tau$), where ξ_τ is the correlation length in the imaginary time direction [31]. In our case $\xi_\tau \sim \exp(A\xi^{1/2})$, which is one manifestation of the critical behavior at the IRFP (i.e. the dynamical exponent formally being $z = \infty$), and $\xi = L$ for a finite system at criticality. Therefore we expect ρ_S to scale as [32]

$$\ln \rho_S(L) \sim -\sqrt{L}. \quad (23)$$

Combining this with Eq.(22), we expect $g(x)$ to behave as a constant $\simeq \pi^{-1}$ in the delocalized regime (i) and to vanish as

$$\ln g(x) \sim -\sqrt{x} \quad (24)$$

in the localized regime (ii).

3.2 Numerical results

Following the method explained in Sec. 2., we study the spin- $\frac{1}{2}$ XX model [Eq.(5)] with random bonds J_i distributed according to the flat distribution

$$\mathcal{P}(J) = \begin{cases} \frac{1}{2W} & \text{if } J \in [1-W, 1+W] \\ 0 & \text{otherwise.} \end{cases}, \quad (25)$$

which implies that the disorder strength is $\mathcal{D} = \frac{1}{3}W^2$. Due to the strong sample-to-sample fluctuations that occur in many disordered quantum systems at low or zero temperatures we have to perform a disorder average over a sufficiently large number of samples. In our calculations the latter ranges from $N_s = 10^3$ for the biggest size up to 10^5 for the smaller ones such that the error bars are well controlled, as we checked carefully. The system sizes vary from $L_{min} = 8$ to $L_{max} = 2048$ and we considered a large range

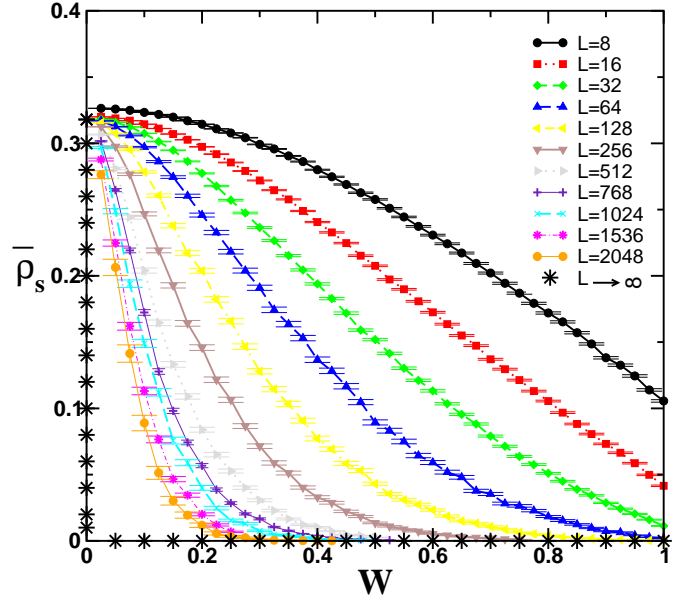


figure 2. Disorder averaged value of the spin stiffness $\overline{\rho}_S$ vs the disorder strength $W \sim \sqrt{\mathcal{D}}$ for different system sizes, as indicated on the plot. Averaging has been done over $N_s = 10^3$ samples for the biggest sizes and up to 10^5 for the smallest ones such that the error bars are well controlled, as we can observe. The expected behavior in the thermodynamic limit is represented by the black stars.

of disorder strengths between $W_{min} = 0.025$ and $W_{max} = 1$. The spin stiffness ρ_S was evaluated using Eq.(17) with a twist angle $\phi = L \times \delta\phi = L \times \pi/10^4$ and was then averaged over N_s independent samples: $\overline{\rho}_S = \frac{1}{N_s} \sum_{\{\text{samples}\}} \rho_S$. In Fig.2 $\overline{\rho}_S(W)$ is shown for different system sizes and we see clearly that it approaches zero for increasing L . In order to validate the FS scaling form [Eq.(23)], we studied the distribution of $\ln \rho_S$. For $W = 0.5$, Fig.3 (a) shows such a distribution for system sizes ranging from 8 to 512 sites with $N_s = 10^4$ samples. As expected for a system described by an IRFP the distribution gets broader with increasing system size, which confirms that the dynamical exponent is formally infinite $z = \infty$. Following Eq.(23), the distribution $P(\frac{\ln \rho_S}{\sqrt{L}})$ is plotted in Fig.3 (b) and as expected, the data of Fig.3 (a) collapse in a universal function.

When the disorder is weaker, we expect strong FS effects and a disorder-dependent length scale might control a crossover between the pure repulsive XX fixed point and the attractive IRFP. Such a behavior is illustrated in Fig.4(a) since $\overline{\rho}_S(L)$ has been calculated for various values of the disorder W . Typically, when $W \geq 0.3$ we can observe the asymptotic behavior $\ln \overline{\rho}_S(L) \sim -L^{1/2}$ as soon as $L \simeq 100$ but when $W < 0.1$ the pure behavior $\overline{\rho}_S \simeq \pi^{-1}$ remains robust up to very large L and even for $L = 2048$ the IRFP asymptotic regime is not yet reached.

In order to characterize this crossover behavior, we studied the scaling function defined by Eq.(22) and a corresponding scaling plot of $-(\ln g(L/\xi^*))^{-1}$ is shown in Fig.4(b). For $W = 0.225$ we have chosen $\xi^* = 100$ such

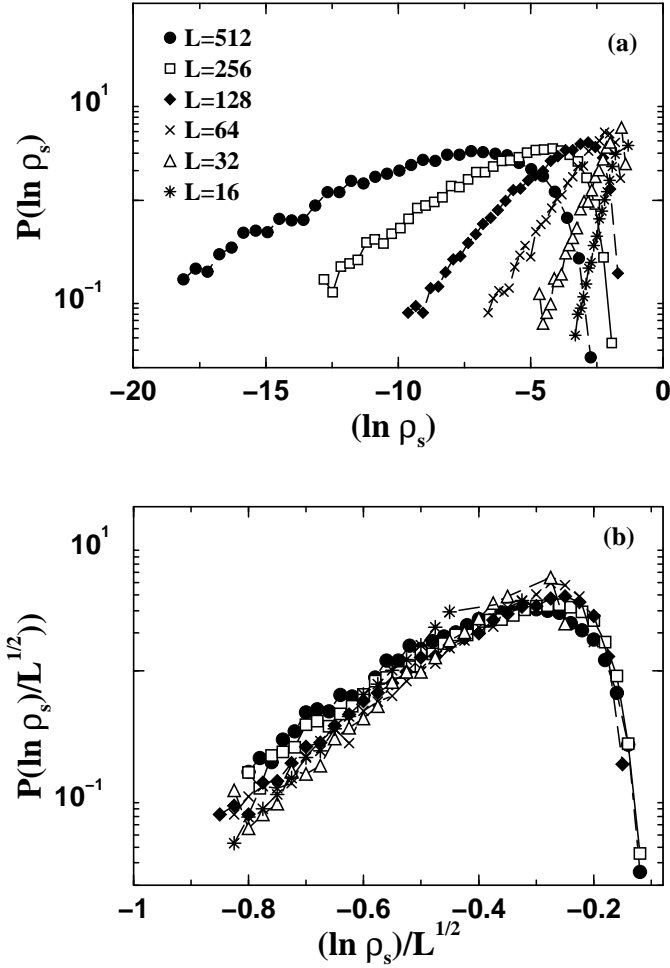


figure 3. Distribution of the spin stiffness obtained with $N_s = 10^4$ samples at $W = 0.5$. The system sizes are indicated on the plot. (a) The distribution of $\ln(\rho_s)$ is broadening with system size. (b) Scaling plot of the data shown in Fig.3 (a), assuming that the logarithm of the stiffness varies as the square root of the system size.

that the crossover region is centered around $x = L/\xi^* \simeq 1$ and the other estimates, indicated on the plot, have been adjusted carefully in order to obtain the best data collapse. The 3 regimes mentioned above (see Sec. 3.1) are clearly visible : The pure regime (i) for which the stiffness takes values close to π^{-1} is observed if $x \ll 1$. When $x \gg 1$ the infinite randomness regime (ii) is relevant : the universality of the IRFP is recovered and $g(x)$ is in perfect agreement with Eq.(24). The intermediate crossover regime (iii) is visible for $x \sim 1$.

4 The localization length as a crossover length scale

Finally, we study the disorder dependence of the localization length ξ^* . Using the values extracted from the data collapse shown in Fig.4(b), $\xi^*(\mathcal{D})$ is shown in Fig.5(a) for

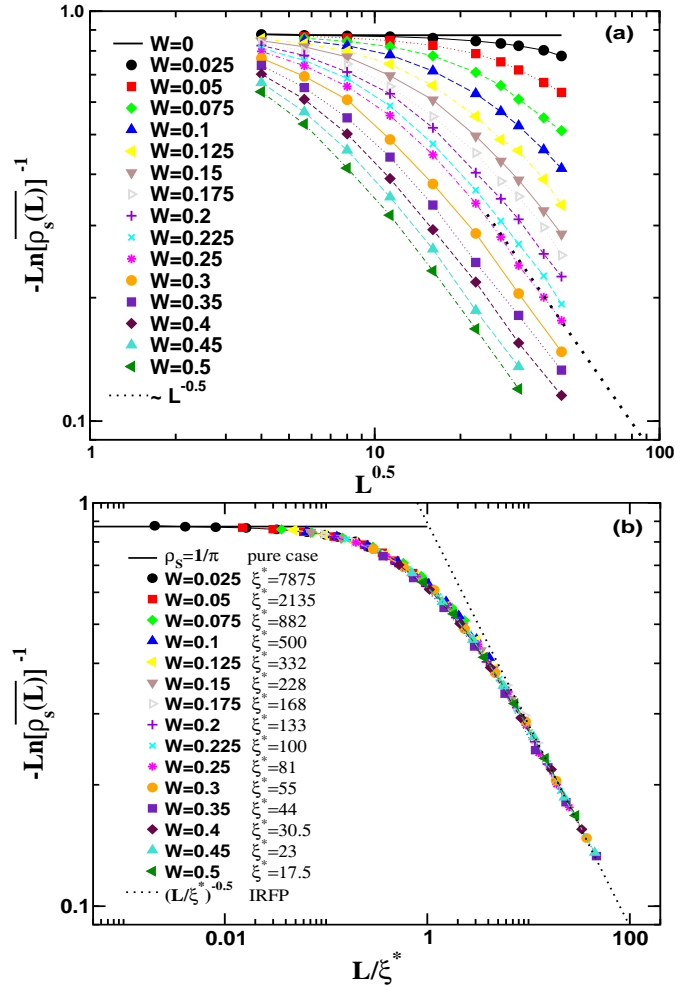


figure 4. (a) Inverse logarithm of the disorder averaged spin stiffness plotted for several box sizes W specified on the plot. The error bars are smaller than symbol sizes. The full line stands for the pure case and the dotted one shows the expected IRFP behavior [Eq.(23)]. (b) Scaling plot according to Eq.(22) of the data shown in Fig.4(a) with ξ^* indicated on the plot for each W . Pure and IRFP behavior are indicated respectively by full and dotted lines.

several values of the disorder strength. The numerical results are compared with the predicted power-law behavior Eq.(21) which is at the XX point given by $\xi^*(\mathcal{D}) \sim \mathcal{D}^{-1}$. The agreement between the numerical results and the bosonization prediction is very good for weak disorder, but for $\mathcal{D} > 0.1$ the data deviate from a power-law. In order to extract a functional form for ξ^* also in this range of disorder we look at its behavior as a function of the variance δ of the random variable $\ln J_i$:

$$\delta = \sqrt{(\overline{\ln J_i})^2 - (\overline{\ln J_i})^2} \quad (26)$$

which is related to W via

$$\delta = \sqrt{1 - \frac{1 - W^2}{4W^2} \left[\ln \left(\frac{1 + W}{1 - W} \right) \right]^2}. \quad (27)$$

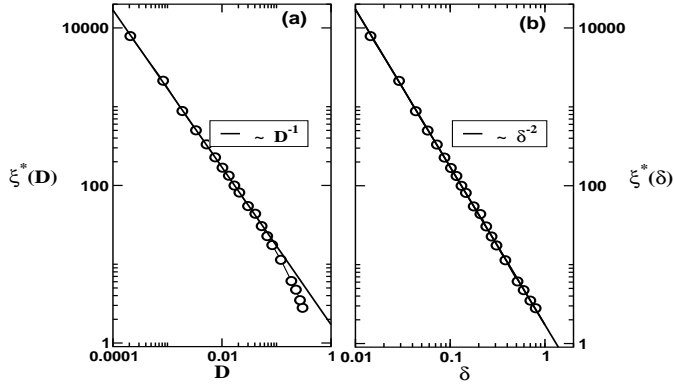


figure 5. Disorder dependence of the localization length ξ^* of the random XX chain. Numerical results are shown with open circles and full lines represent power-laws as indicated on the plot. (a) As a function of the disorder parameter D and (b) as a function of the disorder parameter δ .

As we can observe in Fig.5(b), the parameter δ is very useful to describe the disorder dependence of ξ^* for any strength of randomness, indeed the power-law $\xi^*(\delta) \sim \delta^{-2}$ works perfectly for the whole range of randomness considered here. Hence we assume that Eq.(21) has to be replaced, for strong disorder, by

$$\xi^*(\delta) \sim \delta^{-\Phi}, \quad (28)$$

and since for weak disorder $\delta \sim \sqrt{D}$, we expect $\Phi = \frac{2}{3-2K}$.

Actually, a similar conclusion was drawn in [12,13], where the crossover effects visible in the spin-spin correlation function of random AF spin chains were studied. Indeed the correlation functions of the weakly disordered spin- $\frac{1}{2}$ XXZ chain display a strong crossover behavior controlled by a disorder-dependent crossover length scale ξ which behaves as $\delta^{-1.8 \pm 0.2}$ [12]. In analogy to what we did with the stiffness above, we can extract the crossover length scale ξ using the scaling function

$$\tilde{c}(x) = C_{\text{avg}}(L)/C_0(L), \quad \text{with } x = \frac{L}{\xi}, \quad (29)$$

where $C_0(L)$ and $C_{\text{avg}}(L)$ are spin-spin correlation functions calculated at mid-chain respectively for the pure and random models. At the XX point, when $W = 0$, $C_0(L) \propto L^{-1/2}$ and at the IRFP $C_{\text{avg}}(L) \propto L^{-2}$. The crossover between these two distinct behaviors is shown in Fig.6(a) where $\tilde{c}(x)$ presents a universal form, following $\tilde{c}(x) = \text{constant}$ for $x \ll 1$ and $\tilde{c}(x) \sim x^{-3/2}$ for $x \gg 1$. We see that the characteristic length scale ξ beyond which the asymptotic IRFP behavior sets in in the correlation function scales with disorder strength in very much the same way as the localization length ξ^* .

5 Conclusion

In this paper we have studied the scaling behavior of the stiffness of the random antiferromagnetic spin- $\frac{1}{2}$ XX

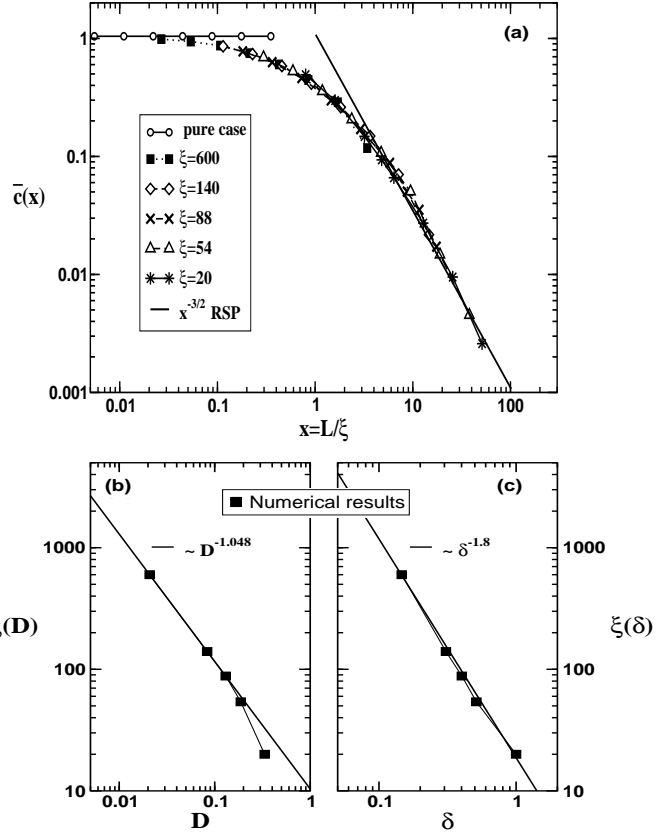


figure 6. (a) Scaling plot according to Eq.(29) of mid-chain xx correlation function data obtained in [12,13] for 5 different values of W indicated on the figure as well as the ξ used for the data collapse. The line with open circles shows the pure behavior and the full line shows the RSP behavior at the IRFP. The crossover length scale ξ is plotted vs D and fitted by $D^{-1.048 \pm 0.1}$ only for weak disorder in (b) whereas in (c) $\xi(\delta)$ displays a better agreement with a power law $\sim \delta^{-1.8 \pm 0.2}$, $\forall \delta$.

chain numerically via exact diagonalization calculations utilizing the fact that the system can be mapped on a free fermion model. The latter allowed us to study rather large system sizes by which we were able to analyze thoroughly the crossover effects observable for weak disorder. Our results clearly show that the asymptotic behavior of the model under consideration is governed by an infinite randomness fixed point for all disorder strengths, including the weakest, as predicted by D. Fisher [30]. We could observe one of the characteristics of the IRFP, namely a formally infinite value for the dynamical exponent, from the finite size scaling behavior of the probability distribution of the stiffness, where $\ln \rho_s/L^{1/2}$ occurs as a scaling variable indicating that the stiffness scales exponentially with the the square root of the system size.

Moreover we showed that the finite size scaling form of the average value of the stiffness is governed by a characteristic length scale that depends on the strength of the disorder. The length scale can be identified as a localization length with regard to transport properties but also as a crossover length scale below which the system be-

has essentially like a pure (disorder free) chain and the stiffness is constant and beyond which the asymptotic behavior characteristic for an infinite randomness fixed point becomes visible and the stiffness scales to zero with a characteristic power of the system size. We found that this length scale diverges like $1/\delta^2$ with decreasing variance δ of the disorder, which agrees well with an analytical prediction using bosonization techniques. This behavior agrees also well with the scaling behavior of the crossover length for the spin-spin correlation function, which indicates that there is indeed a single disorder strength dependent length scale governing the crossover as well as the localization phenomena in this system.

References

1. H. Bethe, Z. Physik **71**, 205 (1931).
2. N. D. Mermin and H. Wagner, Phys. Rev. Lett. **17**, 1133 (1966).
3. C. J. Hamer, G. R. W. Quispel, and M. T. Batchelor, J. Phys. A **20**, 5677 (1987); F. Woynarovich and H.-P. Eckle, J. Phys. A **20**, L97 (1987); F. C. Alcaraz, M. N. Barber, and M. T. Batchelor, Ann. Phys. **182**, 280 (1988).
4. N. Byers and C. N. Yang, Phys. Rev. Lett. **7** 46 (1961).
5. B. S. Shastry, and B. Sutherland, Phys. Rev. Lett. **65**, 243 (1990); B. Sutherland and B. S. Shastry, Phys. Rev. Lett. **65**, 1833 (1990).
6. T.M.R. Byrnes, R.J. Bursill, H.-P. Eckle, C.J. Hamer, and A. W. Sandvik, Phys. Rev. B **66**, 195313 (2002).
7. S. Eggert and I. Affleck, Phys. Rev. B **46**, 10866 (1992); S. Eggert and I. Affleck, Phys. Rev. Lett. **75**, 934 (1995).
8. C. L. Kane and M. P. A. Fisher, Phys. Rev. Lett. **68**, 1220 (1992); **46**, 15 233 (1992).
9. C. A. Doty and D. S. Fisher, Phys. Rev. B **45**, 2164 (1992).
10. E. Abrahams, P. W. Anderson, D. C. Licciardello and T. V. Ramakrishnan, Phys. Rev. Lett. **42**, 673 (1979).
11. T. Giamarchi and H. J. Schulz, Phys. Rev. B **37**, 325 (1988).
12. N. Laflorencie and H. Rieger, Phys. Rev. Lett. **91**, 229701 (2003).
13. N. Laflorencie, H. Rieger, A. W. Sandvik, and P. Henelius, preprint cond-mat/0312572.
14. K. Hamacher, J. Stolze, and W. Wenzel, Phys. Rev. Lett. **89**, 127202 (2002).
15. O. Montrunich, K. Damle, and D. Huse, Phys. Rev. B **63**, 134424 (2001).
16. G. Bouzerar, D. Poilblanc, and G. Montambaux, Phys. Rev. B **49**, 8258 (1994).
17. K. J. Runge and G. T. Zimanyi, Phys. Rev. B **49**, 15212 (1994).
18. T. Giamarchi and B. S. Shastry, Phys. Rev. B **51**, 10915 (1995).
19. P. Schmitteckert et al., Phys. Rev. Lett. **80**, 560 (1998).
20. L. Urba and A. Rosengren, Phys. Rev. B **67**, 104406 (2003).
21. F. Schütz, M. Kollar, and P. Kopietz, Phys. Rev. Lett. **91**, 017205 (2003).
22. I. Affleck and P. Simon, Phys. Rev. Lett. **86**, 2854 (2001); P. Simon and I. Affleck, Phys. Rev. Lett. **89**, 206602 (2002).
23. W. G. van der Wiel et al., Science **289**, 2105 (2000); J. Nygard, D. H. Cobden, and P. E. Lindelof, Nature (London) **408**, 342 (2000).
24. A. P. Young and H. Rieger, Phys. Rev. B **53**, 8486 (1996).
25. E. Lieb, T. Schulz, and D. Mattis, Ann. Phys. (NY) **16**, 407 (1961).
26. N. Laflorencie, S. Capponi and E. S. Sorensen, Eur. Phys. J. B **24**, 77 (2001).
27. The linear algebra package LAPACK has been used here.
28. P. Henelius and S. M. Girvin, Phys. Rev. B **57**, 11457 (1998).
29. F. Igloi, R. Juhász, and H. Rieger, Phys. Rev. B **61**, 11552 (2000).
30. D. S. Fisher, Phys. Rev. B **50**, 3799 (1994).
31. M. Wallin, E. S. Sørensen, S. M. Girvin, and A. P. Young, Phys. Rev. B **49**, 12115 (1994).
32. Strictly speaking there is a logarithmic correction but it is subdominant.